Journal of Magnetic Resonance 293 (2018) 34–40

Contents lists available at ScienceDirect

Journal of Magnetic Resonance

journal homepage: www.elsevier.com/locate/jmr

Boosting sensitivity and suppressing artifacts via multi-acquisition in direct polarization NMR experiments with small flip-angle pulses

Riqiang Fu [a,*], Arturo J. Hernández-Maldonado [b]

[a] National High Magnetic Field Laboratory, Florida State University, 1800 East Paul Dirac Drive, Tallahassee, FL 32310, United States
[b] Department of Chemical Engineering, University of Puerto Rico-Mayagüez Campus, Mayagüez, PR 00681-9000, United States

ARTICLE INFO

Article history:
Received 2 February 2018
Revised 19 May 2018
Accepted 23 May 2018
Available online 24 May 2018

Keywords:
Direct polarization
Multi-acquisition
Adiabatic inversion pulse
Sensitivity enhancement
Small flip-angle pulse

ABSTRACT

A small flip-angle pulse direct polarization is the simplest method commonly used to quantify various compositions in many materials applications. This method sacrifices the sensitivity per scan in exchange for rapid repeating of data acquisition for signal accumulation. In addition, the resulting spectrum often encounters artifacts from background signals from probe components and/or from acoustic rings leading to a distorted baseline, especially in low-γ nuclei and wideline NMR. In this work, a multi-acquisition scheme is proposed to boost the sensitivity per scan and at the same time effectively suppress these artifacts. Here, an adiabatic inversion pulse is first applied in order to bring the magnetization from the +z to −z axis and then a small flip-angle pulse excitation is used before the data acquisition. Right after the first acquisition, the adiabatic inversion pulse is applied again to flip the magnetization back to the +z axis. The second data acquisition takes place after another small flip-angle pulse excitation. The difference between the two consecutive acquisitions cancels out any artifacts, while the wanted signals are accumulated. This acquisition process can be repeated many times before going into next scan. Therefore, by acquiring the signals multiple times in a single scan the sensitivity is improved. A mixture sample of flufenamic acid and 3,5-difluorobenzoic acid and a titanium silicate sample have been used to demonstrate the advantages of this newly proposed method.

1. Introduction

The simplest polarization scheme in nuclear magnetic resonance (NMR) is to apply a single excitation pulse to flip the magnetization away from its equilibrium state in the longitudinal direction (+z axis), as illustrated in Fig. 1a. The projection of the tilted magnetization onto the horizontal plane (the xy plane) generates transverse magnetization which is detected by the receiver. Since all resonances respond uniformly to the flip-angle of the excitation pulse (assuming that the B_1 field across a sample coil generated by the radiofrequency (RF) pulse is uniform), quantification becomes straightforward in such a direct polarization. Nowadays, direct polarization is still commonly used in many materials applications such as catalysts/zeolites, batteries, silicates, etc. [1–7], where either no abundant spin is available in the lattice of the materials to be a source for uniform polarization enhancement or it is crucial to quantify various compositions. It has been known that the maximum signals in this direct polarization scheme are achieved by a 90° pulse, which directly brings the magnetization along the longitudinal direction into the transverse plane for detection. In such 90° pulse excitation experiments, the recycle delay between scans is required to be about five times of the spin-lattice relaxation time (T_1) so that the magnetization could go back to its equilibrium state and thus this polarization scheme can be repeated for signal accumulation in order to improve the signal-to-noise ratio (SNR) and to obtain the quantitative information. However, when T_1 is long, although this 90° pulse excitation gives rise to a maximum signal per scan, it cannot produce a maximum SNR per time unit due to the long recycle delay. In fact, the so-called Ernst-angle pulse excitation [8,9], where the flip-angle and the recycle delay are compromised depending on the T_1 value, yields the optimal sensitivity per time unit. However, for systems where there exist multiple resonances having a large range of T_1 values, such a compromise cannot provide an accurate quantification. For a better quantification, a small flip-angle pulse excitation should always be used due to the following two reasons. (1) A shorter pulse length in general has a broader and more uniform excitation bandwidth in the frequency domain, thus resonances in a very large spectral width could be uniformly polarized [10]. Especially for quadrupolar nuclei, a small flip-angle pulse provides

* Corresponding author.
E-mail address: rfu@magnet.fsu.edu (R. Fu).

https://doi.org/10.1016/j.jmr.2018.05.015
1090-7807/

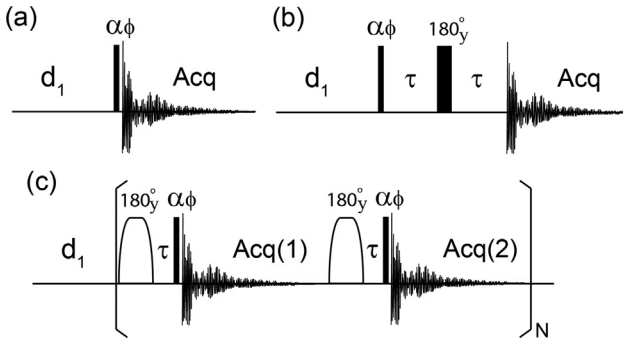

Fig. 1. Pulse sequences used for direct polarization NMR experiments with small flip-angle pulses. The solid rectangles represent hard pulses, while the open shaped pulses stand for adiabatic 180° inversion. The excitation pulse has a flip-angle α with a phase ϕ. Between scans is the recycle delay d_1. (a) Single small flip-angle pulse excitation, where ϕ is (x, −x, y, −y) and the corresponding phase for the receiver is (x, −x, y, −y). (b) Small flip-angle pulse excitation followed by spin-echo refocusing. The phase cycle is listed as ϕ (x, −x, y, −y) and the receiver (x, −x, −y, y). (c) Multi-acquisition scheme, where the phase ϕ is (x, −x, y, −y) and the first receiver phase of (−x, x, −y, y) and the second receiver phase of (x, −x, y, −y). N is the number of loops for repeating these two acquisitions.

a uniform nutation for a large range of quadrupolar interactions [11], which is extremely useful to quantify various species having different quadrupolar coupling constants. (2) The projection of the magnetization along the longitudinal direction after a small flip-angle pulse excitation is very close to its respective equilibrium state and thus could relax back the equilibrium state in a relatively shorter time. However, with a small flip-angle pulse excitation, SNR per scan is low. In addition, as the single-pulse excitation polarizes all signals within the range of the magnetic field generated by the RF pulse, including possible background signals from the probe components outside the sample coil. Moreover, the deadtime ringdown effects, which arise from acoustic rings of the RF pulse right before the receiver opening, often cause a wiggling or distorted baseline in the observed spectra [12], particularly in low-γ nuclei and wideline NMR. These background signals and the wiggling baseline are usually existed in single-pulse excitation spectra. A question to answer is whether or not we can boost the SNR per scan while remaining the advantages of the small flip-angle pulse excitation, and at the same time to suppress those artifacts from these background signals and the deadtime ringdown effects in direct polarization experiments. This query provided the main impetus for the present undertaking.

The spin-echo pulse sequence, as shown in Fig. 1b, is the simplest scheme to suppress the background signals as well as the deadtime ringdown effects. As the data acquisition takes place after a relatively long refocusing delay, any deadtime ringdown effects will be diminished completely. However, the advantages of the small flip-angle pulse excitation cannot be maintained anymore in such spin-echo experiments, because the recycle delay in the experiments has to be five times of the longest T_1 value in all resonances, which will be demonstrated in next section. It was found that in single 90° pulse NMR experiments, the artifacts can be effectively removed [12] by running two experiments one after another without any delay in between, as the first experiment contains the wanted signals as well as the unwanted signals (including background signals and the deadtime ringdown effects), while the second experiment acquires only the unwanted signals, at an expense of lowering the SNR by ~40%. Cross polarization (CP) [13] is another good example for suppressing the deadtime ringdown effects, where the signals of a dilute spin are polarized during a contact time between the protons and the dilute spin when their spin-lock fields fulfill the Hartmann-Hahn matching condition [14]. In the CP experiments, the contact pulse on the dilute spin has the same phase while the receiver's phase is alternated in two consecutive scans. This is because the sign of the cross-polarized signals of the dilute spin can be altered by shifting the phase of the ^{1}H 90° pulse before the CP contact time by 180° that the observed signals of the dilute spin are accumulated in the two scans and the baseline distortion and the background signals from the probe components are effectively suppressing. Here, a new scheme is designed in a similar way to cancel the background signals and the deadtime ringdown effects.

Again, in solid-state CP experiments, a single contact time, during which the spin-lock fields for an abundant spin (such as ^{1}H) and a dilute spin fulfill the Hartmann-Hahn condition, achieves the polarization transfer from ^{1}H to the dilute spin. Since the recycle delay for the CP experiments is governed by the ^{1}H T_1 value, rather than the T_1 values of the dilute spin, repeated contacts between ^{1}H and the dilute spin could be used to transfer the ^{1}H magnetization to the dilute spin multiple times so as to further enhance the signals, in case that the proton spin-lattice relaxation time in the rotating frame ($T_1\rho$) is long enough [13,15]. In this paper, the long spin-lattice relaxation time in the laboratory frame is utilized in a similar way to design a new pulse sequence scheme in order to repeat the signal acquisition multiple times for improving the sensitivity per scan in direct polarization experiments with small flip-angle pulse excitation. A simple vector model will be used to demonstrate the sensitivity enhancement and at the same time to effectively suppress those background signals and the dead time ringdown effects. A mixture of flufenamic acid and 3,5-diflurobenzoic acid samples and a porous titanium silicate sample will be used to illustrate the advantages of this new scheme.

2. Methodology

Fig. 1c shows the pulse sequence used to acquire the signals multiple times in direct polarization experiments with small flip-angle pulse excitation. In the beginning, an adiabatic inversion pulse [16–18] is applied to flip the magnetization from +z to −z direction. After a short delay, a small flip-angle pulse is applied to flip the magnetization away from the −z axis, followed by first data acquisition. At the end of the acquisition, the adiabatic inversion pulse is applied again to bring the magnetization back to +z axis. The same small flip-angle pulse (including its phase) is used to bring the magnetization off the longitudinal direction from the +z axis for acquisition. The phase of the receiver for the second data acquisition is shifted by 180° as compared to the first data acquisition. These two acquisitions can be repeated for N times before going onto the next scan. Since the pulses (the adiabatic inversion pulse and the small flip-angle pulse) before the two acquisitions are identical while the receiver has an opposite phase for the two acquisitions, the probe ringdown effects should be completely canceled in the two consecutive acquisitions.

In order to have a better picture for this multi-acquisition scheme, we use the schematics of the vector presentation, shown in Fig. 2, to explain how the wanted signals from the sample region in the sample coil are enhanced while the background signals from outside the sample coil are suppressed. It is known that an applied RF pulse generates a strong and uniform B_1 field in the sample coil resulting in a flip-angle α, while such a very same RF pulse provides a much weaker and inhomogeneous B_1 field outside the sample coil. As shown in Fig. 2a, when a small flip-angle pulse is applied in Fig. 1a, the wanted magnetization $M_Z^s(0)$ for the signals from inside the sample coil (in blue) is flipped by α from the +z axis, but the unwanted background signals $M_Z^b(0)$ in red from outside the sample coil are just slightly tilted away from the +z axis. The observed signals S_{obs} will be the projections of both $M_Z^s(0)$ and $M_Z^b(0)$ onto the xy plane after these tilts:

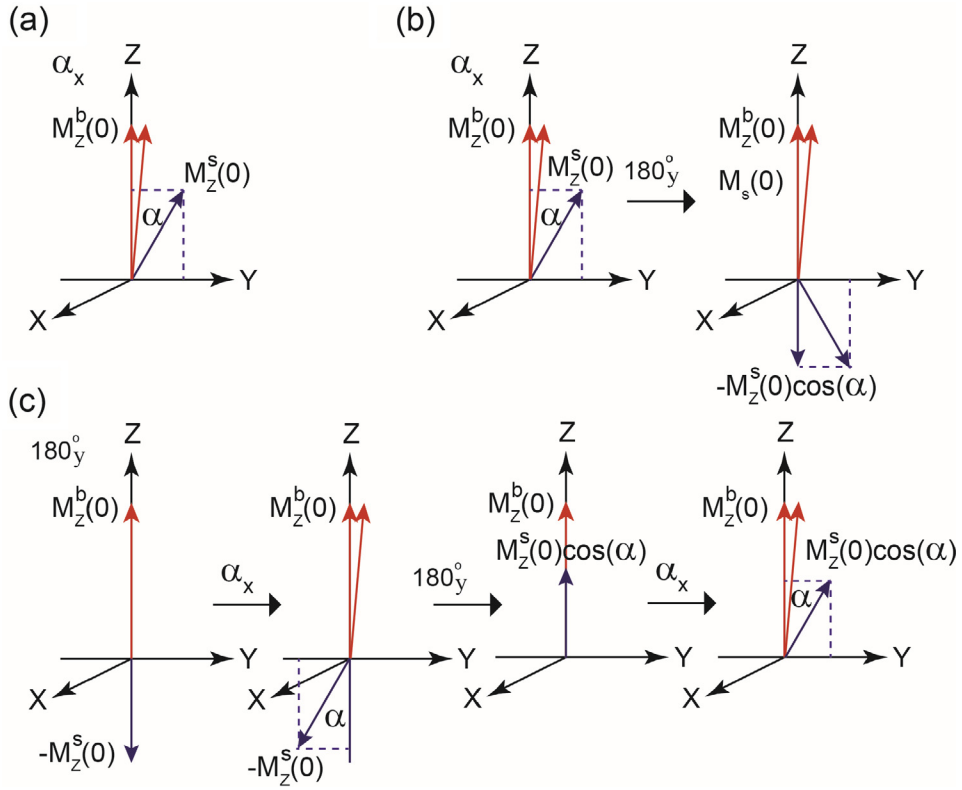

Fig. 2. Schematics of the respective vector presentations in the pulse sequences shown in Fig. 1. Here $M_Z^s(0)$ in blue and $M_Z^b(0)$ in red represent the magnetizations of the signals from inside the sample coil and the background signals from outside the sample coil, respectively. (For interpretation of the references to color in this figure legend, the reader is referred to the web version of this article.)

$$S_{obs} = M_Z^S(0)\sin(\alpha) + M_Z^b(0)\sin(\gamma), \quad (1)$$

where γ stands for the flip-angle that is experienced by the background signals from outside the sample coil, which should be much smaller than α. Since both of them are polarized coherently by the excitation pulse, they will be accumulated with repeated acquisitions. Therefore, the background signals always coexist with the sample signals in the direct polarization NMR experiments. In some cases, the background signals could be much stronger, depending on the materials used in the probe, than the sample signals, making it very difficult to analyze the observed spectra. It is thus always preferable to suppress the background signals. After the acquisition, the signal component in the xy plane relaxes to zero, while the longitudinal component, which is $M_Z^s(0)\cos(\alpha)$, remains. When α is small, this longitudinal component is very close to the equilibrium value of $M_Z^s(0)$. Therefore, it required a much shorter time for this remaining component to relax back to its equilibrium. In other word, the recycle delay can be short to repeat the acquisition for signal accumulation.

The simplest method to suppress the background signals as well as the deadtime ringdown effects is the spin-echo pulse sequence, as shown in Fig. 1b. This is due to the fact that the background signals do not experience the same 180° refocusing pulse as those signals from inside the sample coil, as shown in Fig. 2b, so that they are completely canceled out after the phase cycling. However, for the wanted signals, the longitudinal component $M_Z^s(0)\cos(\alpha)$ along the +z axis after the small flip-angle pulse is inverted by the 180° refocusing pulse to the −z axis. Therefore, the recycle delay should allow the longitudinal component $-M_Z^s(0)\cos(\alpha)$ to relax back to the equilibrium value of $M_Z^s(0)$. For standard spin-echo experiments when α is 90° for maximum signals per acquisition, the recovery begins from zero to the equilibrium. Therefore, when using a small flip-angle pulse in the spin-echo experiments, it is anticipated that the recycle delay used should be even longer than using a 90° pulse. An additional 180° pulse applied at the echo position could flip the magnetization from the −z back to +z axis, so as to maintain the advantage of using a short recycle delay in the small flip-angle pulse experiment. But only one acquisition is performed in each scan.

Fig. 2c shows the vector presentation in the pulse sequence of Fig. 1c. At the beginning, the magnetization $M_Z^s(0)$ (in blue) for the signals from inside the sample coil are inverted from the +z to −z axis by the adiabatic inversion pulse, while the background signals $M_Z^b(0)$ (in red) from outside the sample coil remain in the +z axis due to a much weaker B_1 field they could experience. Thus, with the assumption of no magnetization loss due to the 180° adiabatic inversion, after a small flip-angle pulse, the first observed signals should be

$$S_{obs}(1) = -M_Z^S(0)\sin(\alpha) + M_Z^b(0)\sin(\gamma). \quad (2)$$

At the end of the first acquisition, the adiabatic inversion pulse flips the longitudinal component $-M_Z^s(0)\cos(\alpha)$ back to the +z axis. Similarly, a small flip-angle pulse tilts this component away from the +z axis for detection in the second acquisition:

$$S_{obs}(2) = M_Z^S(0)\cos(\alpha)\sin(\alpha) + M_Z^b(0)\sin(\gamma). \quad (3)$$

Therefore, the difference between these two consecutive acquisitions removes the background signals while sums up the signals from inside the sample coil:

$$S_{obs} = S_{obs}(2) - S_{obs}(1) = M_Z^S(0)\sin(\alpha)[1+\cos(\alpha)]. \quad (4)$$

By comparing with Eq. (1), we notice that the observed signals are enhanced by a factor of $[1+\cos(\alpha)]$ and the background signals

are canceled. It is to note that at the end of the second acquisition, the signal magnetization becomes $M_Z^s(0)\cos^2(\alpha)$ along the +z axis, which remains close to the equilibrium value when α is small, thus requires a shorter time to relax back to the equilibrium state. On the other hand, this orientation of the magnetizations is the same as the initial one, thus these two consecutive acquisitions can be repeated for many times to further enhance the observed signals. After repeating N times, the total signals observed should be

$$S_{obs}^N = M_Z^S(0)\sin(\alpha)[1+\cos(\alpha)]\sum_{i=1}^{N}\cos^{2i-2}(\alpha). \quad (5)$$

Consequently, the sensitivity enhancement factor ε after the N^{th} loop in the multi-acquisition scheme over the single small flip-angle pulse excitation becomes:

$$\varepsilon = \frac{S_{obs}^N}{M_Z^S(0)\sin(\alpha)\sqrt{2N}} = [1+\cos(\alpha)]\sum_{i=1}^{N}\cos^{2i-2}(\alpha)/\sqrt{2N}, \quad (6)$$

where a factor of $\sqrt{2N}$ comes from the noise contributions in a total of 2N acquisitions [19]. While at the end of the N^{th} loop, the magnetization along the longitudinal direction (+z axis) becomes $M_Z^s(0)\cos^{2N}(\alpha)$. The recycle delay d_1 should be used to bring this magnetization back to the equilibrium.

3. Experimental

Flufenamic acid (FFA) and 3,5-difluorobenzoic acid (FBA) were purchased from Sigma-Aldrich and used without further purification. These two samples were physically mixed and packed into a 1.3 mm rotor. All ^{19}F NMR experiments were carried out on a Bruker Avance 600 MHz NMR spectrometer operating at the resonance frequency of 564.68 MHz for ^{19}F using a Bruker HX 1.3 mm MAS probe, in which the ^1H channel was tuned to ^{19}F. The sample spinning rate was controlled by a Bruker pneumatic MAS unit at 40 kHz ± 10 Hz. The ^{19}F 90° pulse length was calibrated to be 2.7 μs and the corresponding power level was used for all hard pulses and adiabatic inversion pulses. The pulse duration of 50 μs was used for the adiabatic inversion, whose waveform was achieved by using a 15% apodized amplitude and 60 kHz chirp frequency sweep [16,17]. In all ^{19}F experiments, 64 scans were used to accumulate the signals. The ^{19}F chemical shift for FFA was set to −61.5 ppm for reference.

4. Results and discussion

Fig. 3a shows the ^{19}F MAS NMR spectrum of the FFA and FBA mixture sample. The narrower resonance at −61.5 ppm belongs to the $-CF_3$ in FFA, while the broader signal at −108 ppm comes from the two fluorine sites in FBA. Since this 1.3 mm Bruker MAS probe was not designed for ^{19}F observations, there exist ^{19}F background signals from the probe components, which could be seen clearly when using an empty rotor (spectrum not shown). Such ^{19}F background signals are reflected in the baseline and still visible in Fig. 3a, even though the sample signals are strong. The T_1 values for FFA and FBA were measured to be 3.11 and 3.07 s, respectively, in separate experiments (spectra not shown). Since a small flip-angle ($\alpha = 30°$) pulse was used, a shorter recycle delay of 3 s was enough to accumulate the signals. However, when the spin-echo sequence was used, the obtained signals were about 30% weaker than that obtained by using the single small flip-angle pulse, as indicated in Fig. 3b, although the background signals were suppressed. This is due to the short recycle delay used in the spin-echo experiments. As discussed earlier, for the spin-echo experiments, the recycle delay used has to be about five times of the T_1 values.

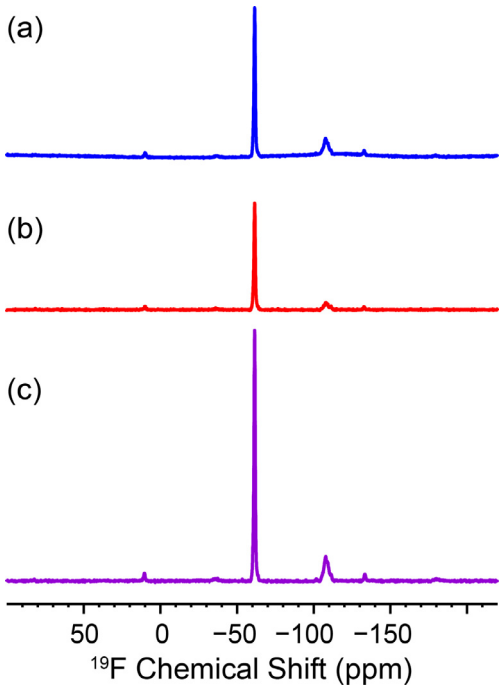

Fig. 3. ^{19}F MAS spectra of the FFA and FBA mixture using different pulse sequences with small flip-angle pulse, as shown in Fig. 1. (a) Direct polarization; (b) spin-echo with $\tau = 25$ μs (a spinning period); (c) multi-acquisition with $\tau = 1$ ms and N = 1. In these experiments, the excitation pulse with a flip-angle of $\alpha = 30°$ was used, and the recycle delay d_1 was set to 3.0 s.

Fig. 3c shows the spectrum recorded by using the multi-acquisition scheme (with N = 1). It can be clearly seen from the spectrum that the signal intensities increase by ~70% in comparison with that in Fig. 3a in the same total experimental time, while the background signals are completely suppressed with no baseline distortion. When the number of loop increased, the observed signal intensities increased further without increasing the total experimental time. As indicated in Table 1, when N = 4, the observed signal intensities increase by a factor of 4. Fig. 4 shows the ^{19}F signals obtained using the pulse sequences in Fig. 1a and c. Clearly, the signal intensities steadily increase as more data acquisitions are used in the multi-acquisition scheme. However, it is expected that more noise would also be recorded with more data acquisitions. Therefore, SNR would become lower when the gain in signal intensities is less than the increase in the noise level.

Since the relative signal intensities between FFA and FBA obtained by using Fig. 1c with different loop number N and different flip-angle α are the same as that by using Fig. 1a, due to their similar T_1 value, Table 1 lists only the signal intensity for the peak at −61.5 ppm from FFA obtained by Fig. 1c, as normalized to that signal acquired by Fig. 1a. When the flip-angle α was 30° and 20°, the experimentally obtained SNR reached its maximum of ~142% when N = 3. While at a smaller flip-angle α at 10°, the experimentally obtained SNR reached the maximum of ~187% when N = 5. On the other hand, the calculated ε from Eq. (6) suggest a maximal of 180% for $\alpha = 30°$, of 243% at N = 5 for $\alpha = 20°$, and of 293% at N = 5 for $\alpha = 10°$. The calculated ε's are always larger than the experimentally measured ones, but they seem to have a similar dependence with the number of loops. It is worth to note that Eq. (6) is based on the assumption that there is no magnetization loss during the adiabatic inversion. In practice, the inversion can hardly be perfect. The more inversion pulses are applied, the more magnetization is lost, which would lead to a larger calculated ε than the observed one. Another reason for the discrepancy is the recycle delay used for magnetization recovery. The recycle delay d_1

Table 1
The ^{19}F NMR signal intensity of FFA obtained in the multi-acquisition scheme as compared to that in the one pulse excitation.

α		Multi-acquisition scheme				
		N = 1	N = 2	N = 3	N = 4	N = 5
30°	Signal Intensity	1.69	2.78	3.52	4.05	n/a
	SNR	1.20	1.39	1.43	1.43	n/a
	Calculated ε	1.32	1.63	1.76	1.80	1.80
20°	Signal Intensity	1.69	2.79	3.49	4.00	4.36
	SNR	1.20	1.40	1.42	1.41	1.39
	Calculated ε	1.37	1.83	2.11	2.30	2.43
10°	Signal Intensity	1.85	3.25	4.32	5.20	5.91
	SNR	1.31	1.63	1.76	1.84	1.87
	Calculated ε	1.40	1.95	2.36	2.68	2.93

Note: All signal intensities were normalized to that obtained in the one pulse excitation with their respective flip-angle α. SNR is obtained by the observed signal intensity divided by $\sqrt{2N}$, while the calculated sensitivity enhancement factor ε is based on Eq. (6) with the assumption of no magnetization loss during the adiabatic inversion pulses.

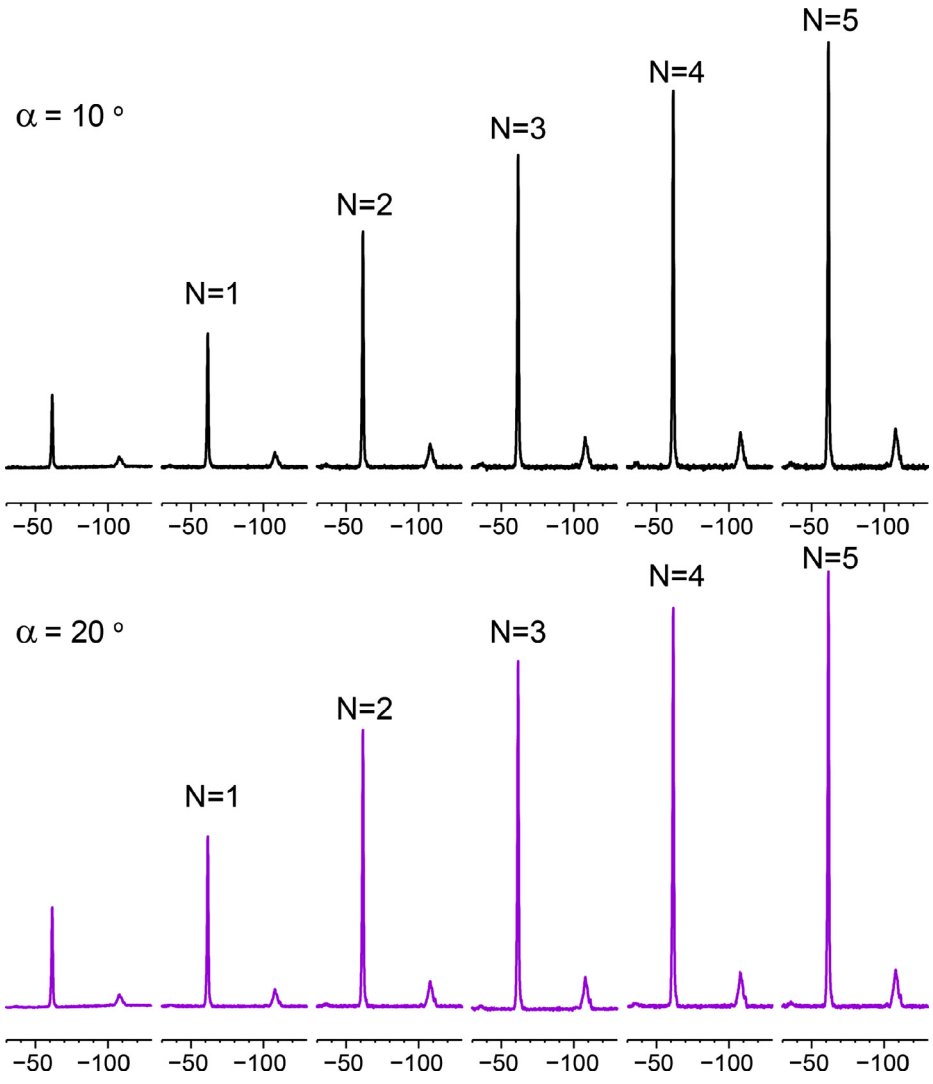

Fig. 4. Comparison of the ^{19}F signals obtained using the pulse sequences in Fig. 1a and c at different flip-angle pulse. (Top) α = 10° and d_1 = 1.0 s; (Bottom) α = 20° and d_1 = 2.0 s. The first spectra in the left were obtained with a small flip-angle pulse in Fig. 1a and the other spectra were recorded using the multi-acquisition scheme in Fig. 1c with different loop numbers.

is supposed to bring the magnetization of $M_Z^s(0)\cos^{2N}(\alpha)$ after the end of the Nth loop back to its equilibrium, which should depend on the flip-angle α and the number of loops N. When α = 30°, after 3rd loop, the remaining magnetization is scaled by $\cos^6(30^\circ) = 0.423$. Therefore, the recycle delay of 3 s, which was calibrated using the pulse sequence in Fig. 1a, would not be long enough to bring this magnetization back to its equilibrium. Instead, this recycle delay could only establish a pseudo-equilibrium state, which is less than $M_Z^s(0)$. However, when the flip-angle α is small (e.g. 10°), the remaining magnetization is scaled by $\cos^6(10^\circ) = 0.9122$, which requires a much shorter time for the magnetization going back to its equilibrium. In particular, for quantitative measurements in

systems where T_1 varies in a large range, caution to set up the experimental conditions has to be taken, since both the loop number N and the pulse flip-angle α affect the remaining magnetization position (i.e. $M_Z^s(0)\cos^{2N}(\alpha)$) after the end of the N^{th} loop. For a better quantification, the recycle delay has to be long enough to bring the magnetization from $M_Z^s(0)\cos^{2N}(\alpha)$ back to equilibrium for all T_1 sites. In general, a smaller α would make $\cos^{2N}(\alpha)$ closer to 1 for better quantitative measurements. Therefore, it is anticipated that this multi-acquisition scheme is particularly useful for a very small flip-angle pulse excitation and with systems having very long T_1.

As an example, we use this multi-acquisition method to obtain ^{29}Si NMR spectrum of a titanium silicate porous adsorbent, abbreviated as UPRM-5, developed by Hernandez-Maldonado and coworkers [20–22]. This material exhibits a flexible framework that produces a large surface area and, when decorated with strontium, interactions to selectively capture CO_2 in from gas mixtures in superior amounts. Since the T_1 of ^{29}Si in silicates may be rather long in certain cases (up to several thousand seconds) and differ for different Si sites in the sample [23], a small flip-angle pulse and a relatively long recycle delay are typically used in experiments in order to obtain quantitative proportions of various structurally distinct Si sites. Here, we used a 10° flip-angle pulse and a recycle delay of 15 s to record the ^{29}Si NMR spectra of the UPRM-5 sample on a Bruker Avance 600 MHz NMR spectrometer using a 4 mm Bruker double-resonance MAS probe. 256 scans were used to accumulate the signals with a total experimental time of ~1 h in all measurements. Fig. 5 shows the ^{29}Si MAS NMR spectra of the UPRM-5 sample at room temperature using different experimental schemes. The spectra shows two resonances at −93 and −97 ppm, corresponding to Si(2Si,2Ti_{oct}) and Si(2Si,1$Ti_{semi\text{-}oct}$) silicon environs, respectively, indicating a mix of five- and six-coordinated titanium atoms in the coordinate framework [24]. Fig. 5a shows the ^{29}Si MAS spectrum of the UPRM-5 sample obtained with the small flip-angle (α = 10°) direct polarization scheme in Fig. 1a, from which the SNR of 16.8 was measured for the peak at −93 ppm. It can also be noticed from the spectrum that the baseline was slightly distorted due to the deadtime ringdown effects. When using the multi-acquisition scheme, as shown in Fig. 5b-d, the sensitivity steadily improves as the number of loops increases, but the relative intensities between the two peaks remain the same as in Fig. 5a. The measured SNR from the spectrum was 24.6, 30.4, and 35.4 when N was set to 2, 4, and 8, respectively, which increased by 146%, 181%, and 211%, respectively, as compared to the spectrum in Fig. 5a, using the same total experimental time. In addition, the deadtime ringdown effects appear to be suppressed effectively in the multi-acquisition scheme and the spectra from Fig. 5b-d do not show any baseline distortion.

5. Conclusion

It has been demonstrated that a multi-acquisition scheme provides an efficient way to boost the sensitivity per scan and at the same time to suppress the background signals and baseline distortion in direct polarization NMR experiments using small flip-angle pulses. Similar multi-acquisitions have been developed in solid-state NMR. For instance, the multi-contact CP experiments [13,15] utilize a relatively long spin-lattice relaxation time in the rotating frame ($T_{1\rho}$) from an abundant spin (e.g. ^{1}H) to make multiple CP contact between the abundant spin and the dilute spin being observed, such that the dilute spin is polarized and detected multiple times within a scan. While in echo-train acquisition experiments [25–29], which take advantages of long spin-spin relaxation time (T_2), multiple acquisitions take place repeatedly when the signals are refocused to enhance the sensitivity. In this newly proposed multi-acquisition scheme, the magnetization from samples inside a sample coil is inverted repeatedly between the −z and +z axis due to a long spin-lattice relaxation time (T_1), providing

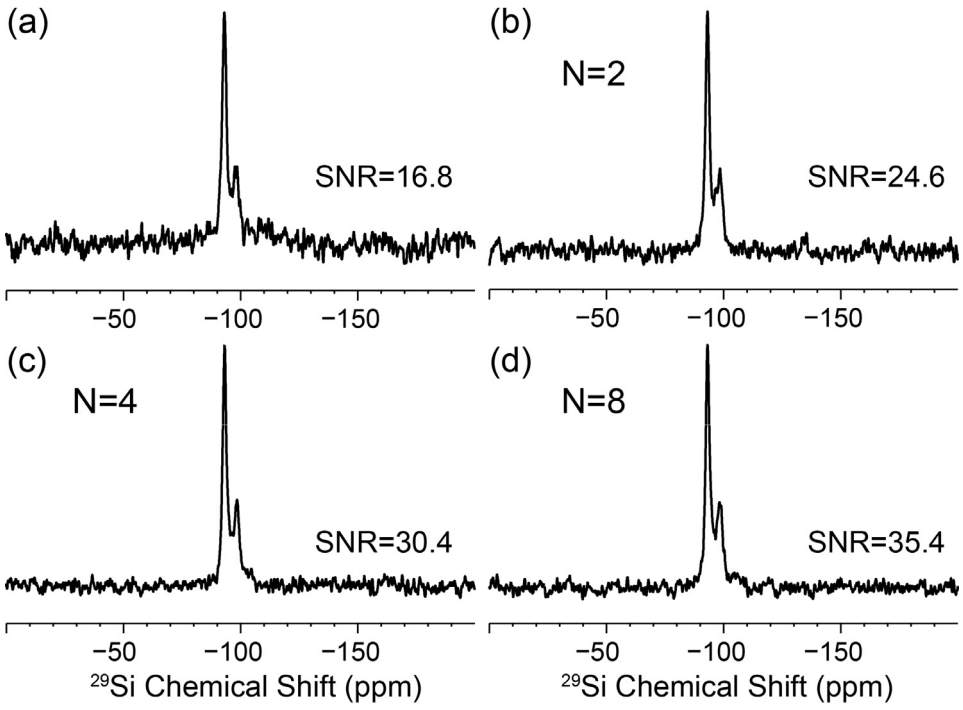

Fig. 5. ^{29}Si MAS NMR spectra of the UPRM-5 sample by using the small flip-angle pulse excitation (a) in Fig. 1a and the multi-acquisition scheme (b-d) in Fig. 1c. The spectra were recorded at room temperature on a Bruker Avance 600 MHz NMR spectrometer using a 4 mm Bruker HX MAS NMR probe. The spinning rate was 8 kHz ± 3 Hz. 256 scans were used to accumulate the signals with a recycle delay of 15 s using a flip-angle of α = 10°. The pulse duration of 100 μs was used for the adiabatic inversion, whose waveform was achieved by using a 15% apodized amplitude and 40 kHz chirp frequency sweep. An exponential window function of LB = 50 Hz was used for the data processing. The chemical shift was referenced to 4,4-dimethy-4-silapentanesulfonate sodium (DSS) at 0 ppm. The measured SNRs are indicated in the spectra.

a mechanism to alter the sign of the sample signals being observed, so that the subtraction adds up the wanted signals multiple times that come from between the magnetization from the −z and +z axis, while suppresses those unwanted background signals from outside the sample coil as well as the deadtime ringdown effects, which are not subjected to the alternation between the −z and +z axis. It is to note that this method highly depends on the performance of the inversion pulse prior to the small flip-angle pulses. For spin-1/2 nuclei, such an adiabatic inversion between the +z and −z directions is quite effective. But for quadrupolar nuclei, the inversion may be complicated in systems where a large range of quadrupolar coupling constants exist [30]. Compared to the CPMG-like echo approaches, this would have great advantages for NMR measurements in systems where a total echo cannot be used due to short T_2 values or inability to refocus all interactions. This new method is particularly useful for spin-1/2 nuclei in materials applications at higher fields and lower temperatures, where the spin-lattice relaxation time could become very long due to highly restricted motions associated with the materials. Therefore, it is anticipated that this new multi-acquisition method offers an opportunity to obtain quantitative proportions of various structurally distinct sites with improved sensitivity in the materials application at high field NMR and at low temperature such as under DNP conditions.

Acknowledgment

All NMR experiments were carried out at the National High Magnetic Field Lab (NHMFL) supported by the NSF Cooperative agreement no. DMR-1644779 and the State of Florida. We also wish to acknowledge support from the Puerto Rico Institute for Functional Materials NSF Award No. EPS-1002410. We gratefully acknowledge helpful comments of a referee for further improving our manuscript.

References

[1] O.B. Lapina, Modern ssNMR for heterogeneous catalysis, Catal. Today 285 (2017) 179–193.
[2] B.E.G. Lucier, Y.N. Huang, Reviewing Ti-47/49 solid-state NMR spectroscopy: from alloys and simple compounds to catalysts and porous materials, Annu. Rep. NMR Spectrosc. 88 (2016) 1–78.
[3] A. Marchetti, J.E. Chen, Z.F. Pang, S.H. Li, D.S. Ling, F. Deng, X.Q. Kong, Understanding surface and interfacial chemistry in functional nonomaterials via solid-state NMR, Adv. Mater. 29 (2017) 1605895.
[4] O. Pecher, J. Carretero-Gonzalez, K.J. Griffith, C.P. Grey, Materials' methods: NMR in battery research, Chem. Mater. 29 (2017) 213–242.
[5] A.G.M. Rankin, P.B. Webb, D.M. Dawson, J. Viger-Gravel, B.J. Walder, L. Emsley, S.E. Ashbrook, Determining the surface structure of silicated alumina catalysts via isotopic enrichment and dynamic nuclear polarization surface-enhanced NMR spectroscopy, J. Phys. Chem. C 121 (2017) 22977–22984.
[6] E. Pump, J. Viger-Gravel, E. Abou-Hamad, M.K. Samantaray, B. Hamzaoui, A. Gurinov, D.H. Anjum, D. Gajan, A. Lesage, A. Bendjeriou-Sedjerari, L. Emsley, J. M. Basset, Reactive surface organometallic complexes observed using dynamic nuclear polarization surface enhanced NMR spectroscopy, Chem. Sci. 8 (2017) 284–290.
[7] D.A. Hirsh, A.J. Rossini, L. Emsley, R.W. Schurko, Cl-35 dynamic nuclear polarization solid-state NMR of active pharmaceutical ingredients, Phys. Chem. Chem. Phys. 18 (2016) 25893–25904.
[8] R.R. Ernst, Sensitivity enhancement in magnetic resonance, Adv. Magn. Reson. 2 (1966) 1–135.
[9] A. Ross, M. Salzmann, H. Senn, Fast-HMQC using Ernst angle pulses: an efficient tool for screening of ligan binding to target proteins, J. Biomol. NMR 10 (1997) 389–396.
[10] R.W. Schurko, Ultra-wideline solid-state NMR spectroscopy, Acc. Chem. Res. 46 (2013) 1985–1995.
[11] A. Samoson, E. Lippmaa, 2D NMR nutation spectroscopy in solids, J. Magn. Reson. 79 (1988) 255–258.
[12] C. Jaeger, F. Hemmann, EASY: A simple tool for simultaneously removing background, deadtime and acoustic ringing in quantitative NMR spectroscopy – Part 1: Basic principle and applications, Solid State Nucl. Magn. Reson. 57–58 (2014) 22–28.
[13] A. Pines, M.G. Gibby, J.S. Waugh, Proton-enhanced NMR of dilute spins in solids, J. Chem. Phys. 59 (1973) 569–590.
[14] S.R. Hartmann, E.L. Hahn, Nuclear double resonance in rotating frame, Phys. Rev. 128 (1962) 2042–2053.
[15] E.O. Stejskal, J.D. Memory, High Resolution NMR in the Solid State – Fundamentals of CP/MAS, Oxford University Press, Oxford, 1994.
[16] R. Fu, G. Bodenhausen, Broadband decoupling in NMR with frequency-modulated "chirp" pulses, Chem. Phys. Lett. 245 (1995) 415–420.
[17] E. Kupce, R. Freeman, Adiabatic pulses for wide-band inversion and broad-band decoupling, J. Magn. Reson. 115 (1995) 273–276.
[18] K.J. Harris, A. Lupulescu, B.E.G. Lucier, L. Frydman, R.W. Schurko, Boradband adiabatic inversion pulses for cross polarization in wideline solid-state NMR spectroscopy, J. Magn. Reson. 224 (2012) 38–47.
[19] M.H. Levitt, Spin Dynamics: Basics of Nuclear Magnetic Resonance, second ed., John Wiley & Sons Ltd, 2008.
[20] J.N. Primera-Pedrozo, B.D. Torres-Cosme, M.E. Clardy, M.E. Rivera-Ramos, H. Hernandez-Maldonado, Titanium silicate porous materials for carbon dioxide adsorption: synthesis using a structure directing agent, detemplation and inclusion of alkaline earth metal cations, Ind. Eng. Chem. Res. 49 (2010) 7515–7523.
[21] J.N. Primera-Pedrozo, S. Dugar, M.M. Martínez-Iñesta, R. Fu, A.J. Hernández-Maldonado, Determination of the apparent crystal structure of a highly faulted UPRM-5 type flexible porous titanium silicate via a polymorph based superposition model, a Rietveld Refinement and a pair distribution function, J. Phys. Chem. C 118 (2014) 8859–8867.
[22] M. Yu, J.N. Primera-Pedrozo, M.E. Marcano-González, A.J. Hernández-Maldonado, Selective adsorption of N_2 over CH_4 in flexible Sr^{2+}- and Ba^{2+}-UPRM-5 (TEA) titanium silicates: effect of activation temperature, Chem. Eng. J. 252 (2014) 311–319.
[23] G. Engelhardt, D. Michel, High-Resolution Solid-State NMR of Silicates and Zeolites, Wiley, Chichester, 1987.
[24] J.N. Primera-Pedrozo, K.J. Guerrero-Medina, R. Fu, H. Hernandez-Maldonado, Sr(II)-UPRM-5 titanium silicate framework thermally induced contraction: *in situ* high temperature XRD and 29Si MAS NMR, Dalton Trans. 40 (2011) 3547–3552.
[25] Mansfield, Multi-plannar image formation using NMR spin echoes, J. Phys. C 10 (1977) L55–L58.
[26] S. Meiboom, D. Gill, Modified spin-echo method for measuring nuclear relaxation times, Rev. Sci. Instrum. 29 (1958) 688–691.
[27] F.H. Larsen, J. Skibsted, H.J. Jakobsen, N.C. Nielsen, Solid-state QCPMG NMR of low-g quadrupolar metal nuclei in natural abundance, J. Am. Chem. Soc. 122 (2000) 7080–7086.
[28] J.H. Baltisberger, B.J. Walder, E.G. Keeler, D.C. Kaseman, K.J.D. Sanders, P.J. Grandinetti, Communication: phase incremented echo train acquisition in NMR spectroscopy, J. Chem. Phys. 136 (2012) 211104.
[29] E.W. Randall, A.A. Samoilenko, R. Fu, Hahn-echoes from ^{14}N in solids by the stray-field method: prospects for imaging using long echo-train summation, Solid State Nucl. Magn. Reson. 14 (1999) 173–179.
[30] C. Jaeger, F. Hemmann, EASY: a simple tool for simultaneously removing background, deadtime and acoustic ringing in quantitative NMRspectroscopy. Part II: Improved ringing suppression, application to quadrupolar nuclei, cross polarisation and 2D NMR, Solid State Nucl. Magn. Reson. 63–64 (2014) 13–19.